

Quiescence Preconditioned Human Multipotent Stromal Cells Adopt a Metabolic Profile Favorable for Enhanced Survival under Ischemia

ADRIEN MOYA,^a NATHANAËL LAROCLETTE,^a JOSEPH PAQUET,^a MICKAEL DESCHEPPER,^a MORAD BENSIDHOUM,^a VALENTINA IZZO,^{b,c,d,e} GUIDO KROEMER,^{b,c,d,e,f,g,h} HERVÉ PETITE,^a DELPHINE LOGEART-AVRAMOGLU^a

Key Words. Human mesenchymal stromal cells • Quiescence • Cell survival • Ischemia • Cell metabolism • Autophagy

^aLaboratory of Bioengineering and Bioimaging for Osteo-Articular tissues, UMR 7052, CNRS, Paris Diderot University, Sorbonne Paris Cité, Paris, France; ^bEquipe 11 labellisée par la Ligue contre le Cancer, Centre de Recherche des Cordeliers, Paris, France; ^cCell Biology and Metabolomics platforms, Gustave Roussy Comprehensive Cancer Center, Villejuif, France; ^dINSERM, U1138, Paris, France; ^eUniversité Paris Descartes, Sorbonne Paris Cité, Paris, France; ^fUniversité Pierre et Marie Curie, Paris, France; ^gPôle de Biologie, Hôpital Européen Georges Pompidou, AP-HP, Paris, France; ^hDepartment of Women's and Children's Health, Karolinska Institute, Karolinska University Hospital Q2:07, Stockholm, Sweden

Correspondence: Delphine Logeart-Avramoglou, Ph.D., Laboratory of Bioengineering and Bio-imaging for Osteo-Articular tissues, UMR 7052 CNRS, Paris Diderot University, 10 Avenue de Verdun, Paris 75010, France. Telephone: +33(0)1 57 27 85 63; Fax: +33(0) 1 57 27 85 71; e-mail: delphine.logeart@univ-paris-diderot.fr

Received January 8, 2016; accepted for publication August 21, 2016; first published online in *STEM CELLS EXPRESS* August 31, 2016.

© AlphaMed Press
1066-5099/2016/\$30.00/0

<http://dx.doi.org/10.1002/stem.2493>

ABSTRACT

A major impediment to the development of therapies with mesenchymal stem cells/multipotent stromal cells (MSC) is the poor survival and engraftment of MSCs at the site of injury. We hypothesized that lowering the energetic demand of MSCs by driving them into a quiescent state would enhance their survival under ischemic conditions. Human MSCs (hMSCs) were induced into quiescence by serum deprivation (SD) for 48 hours. Such preconditioned cells (SD-hMSCs) exhibited reduced nucleotide and protein syntheses compared to unpreconditioned hMSCs. SD-hMSCs sustained their viability and their ATP levels upon exposure to severe, continuous, near-anoxia (0.1% O₂) and total glucose depletion for up to 14 consecutive days in vitro, as they maintained their hMSC multipotential capabilities upon reperfusion. Most importantly, SD-hMSCs showed enhanced viability in vivo for the first week postimplantation in mice. Quiescence preconditioning modified the energy-metabolic profile of hMSCs: it suppressed energy-sensing mTOR signaling, stimulated autophagy, promoted a shift in bioenergetic metabolism from oxidative phosphorylation to glycolysis and upregulated the expression of gluconeogenic enzymes, such as PEPCK. Since the presence of pyruvate in cell culture media was critical for SD-hMSC survival under ischemic conditions, we speculate that these cells may utilize some steps of gluconeogenesis to overcome metabolic stress. These findings support that SD preconditioning causes a protective metabolic adaptation that might be taken advantage of to improve hMSC survival in ischemic environments. *STEM CELLS* 2017;35:181–196

SIGNIFICANCE STATEMENT

Poor survival of grafted cells at the injury site is the major impediment for developing successful cell based therapies. While some studies have focused on improving cell survival upon implantation, most of them have failed to address the critical issue of long term cell survival postimplantation thus drastically reducing the potential benefit of these therapies. In this study, we demonstrated that cellular quiescence preconditioning is a simple, safe, yet very efficient solution for enhancing cell survival in ischemia that may be applicable not only for adult stem cells (hMSC) but also other cell types.

INTRODUCTION

Multipotent stromal cells/mesenchymal stem cells (MSCs) play a key role in the maintenance of tissue integrity and in tissue repair [1, 2]. MSCs have major potential for cell therapy and regenerative medicine applications. A major impediment to the development of MSC-based therapies, however, is poor cell survival and engraftment at the site of injury. The MSC fate may be influenced by cytokines present during the inflammatory response to biomaterials used for implantation, and to

injury itself. However, a prominent explanation for the limited cell survival is the harsh avascular microenvironment that MSCs experience after implantation [3–6]. It is believed that the ischemic milieu, (lack of both nutrients and oxygen supplies) causes MSC death in situ [7]. Thus, limited or absent access to both oxygen and nutrients inevitably disrupts cell metabolism, thereby compromising the function and survival of implanted MSCs.

Because cell survival should enhance the effectiveness of MSC-based therapy, strategies to alleviate massive cell death might be of

prime importance for tissue engineering (TE). Several strategies have been proposed and examined in order to enhance the capability of MSCs to withstand the rigors of the ischemic milieu albeit with limited success [8]. Some strategies focused on the acceleration of vascularization of TE constructs by incorporating pro-angiogenic factors [9–11], while others pharmacologically pre-treated MSCs, or combined MSCs with growth factors (such as tethered EGF) immobilized on matrices, to stimulate pro-survival signaling pathways [12–16]. Recently, a novel strategy developed by our research group countered the conditions of the ischemic environment by exogenously delivering glucose, a main “metabolic fuel” source for cells; this approach strikingly improved the viability of the human MSCs (hMSCs) contained in TE constructs both in an *in vitro* ischemic cell model and in an *in vivo* animal model [17, 18]. Although promising, this approach requires sustained delivery of glucose, rendering its practical implementation difficult.

An alternative strategy to prevent the lethal effects of a compromised metabolic milieu consists in lowering the energy demands of the implanted cells. We speculated that this outcome could be attained by driving the cells toward a quiescent state. In fact, quiescence is characterized by exit from the cell cycle and profound reductions of the metabolic rate that cells, particularly stem cells, adopt in their niche to preserve their key features [19]. In the present study, we examined the hypothesis that preconditioning hMSCs into a quiescent state may contribute to their long-term viability under ischemic conditions. In response to serum deprivation (SD), hMSCs displayed a quiescent profile with reduced ATP-consuming functions. hMSC quiescence contributed to the maintenance of viable and functional hMSCs in both near-anoxia (0.1% O₂) and absence of glucose for up to 14 consecutive days of culture as well as enhanced their survival *in vivo* after subcutaneous implantation in mice. We further investigated the underlying mechanisms of such effects by assessing the metabolic profile of quiescent, preconditioned hMSCs.

MATERIALS AND METHODS

Cells and Cell Culture

Human MSCs were harvested from bone marrow obtained as discarded tissue during routine bone surgery from five adult donors at Lariboisiere Hospital (Paris, France). The tissues were collected with the respective patient’s consent in agreement with Lariboisiere Hospital regulations. hMSCs were isolated from each patient’s bone marrow using a procedure adapted from literature reports [20], characterized (regarding CD markers and differentiation potential; Supporting Information 1), and pooled at an equal ratio at passage 1. These cells were cultured in Alpha Minimum Essential Medium (α MEM; Sigma-Aldrich, St Quentin Fallavier, France, <http://sigmaaldrich.com>) supplemented with 10% Fetal Bovine Serum (FBS; PAA Laboratories, Les Mureaux, France, <http://www.gelifesciences.com>) under an humidified, 37°C, 5% CO₂, environment). hMSCs up to passage 8 were used for the experiments.

Quiescence Preconditioning of hMSCs by Serum Deprivation

hMSCs were seeded at 10⁴ cells per cm² and cultured under standard conditions overnight. The following day, referred to as day-2

(D-2), cells were rinsed with phosphate buffered saline (PBS) and further cultured in α -MEM without FBS for 48 hours. At that time point, referred to as day 0 (D0), preconditioned cells (SD-hMSCs) were ready for either analysis or further experiments. Unpreconditioned hMSC (UP-hMSCs) which were seeded at 10⁴ cells per cm² on day before (D-1) were used as controls.

Ischemic Culture Conditions

The “ischemic” microenvironment was simulated *in vitro* by culturing the hMSCs under both near-anoxia (0.1% O₂) and nutrient (including both serum and glucose) deprivation. Three experimental groups were tested: (a) SD-hMSCs-gluc(–) cultured under ischemic conditions; (b) UP-hMSCs-gluc(–) cultured under ischemic conditions (negative control); and (c) UP-hMSCs-gluc(+) cultured in near-anoxia but in the presence of glucose (positive control). The near-anoxic conditions were achieved, and maintained, using a finely-controlled proOx-C-chamber system (C-Chamber, C-374, Biospherix, New-york, NY, <http://www.biospherix.com>) plus a gas mixture composed of CO₂ and nitrogen. The temperature was maintained at 37°C. At D0, all hMSCs were rinsed with PBS and then cultured in either glucose-free α -MEM (PAN Biotech, Aidenbach, Germany <http://www.pan-biotech.com>; for the gluc(–) groups) or α -MEM containing 5 g/l of glucose (for the gluc(+) group) under near-anoxic conditions without medium change. A set of ischemic culture experiments was specifically conducted using either a pyruvate- and glucose-free or a pyruvate-free supplemented with glucose (5 g/l) Dulbecco’s modified Eagle Medium (DMEM) culture medium (LifeTechnologies, Saint Aubin, France, <https://www.thermofisher.com>).

Cell Cycle Analysis

The respective cell cycle was determined by staining hMSCs with nucleic acid stain Hoechst 33342 (HE; Sigma, Sigma-Aldrich, St Quentin Fallavier, France, <http://sigmaaldrich.com>). Briefly, cells were treated with 1 μ g/ml HE at 37°C for 15 minutes. The stained cells were analyzed using an Attune flow Cytometer (LifeTechnologies, Saint Aubin, France, <https://www.thermofisher.com>; 405/430-470 nm ex./em.). Cell cycle analysis was performed using Attune software (LifeTechnologies, Saint Aubin, France, <https://www.thermofisher.com>). “Resting” cells (at the G0/G1 phase) were identified by the number of cells with 2n DNA while cells that possessed more than 2n DNA were identified as “proliferating” cells (in the S + G2 phase); these results were expressed as a fraction of the total cell population.

Analysis of DNA, RNA and Protein Synthesis

DNA synthesis was monitored using the Click-iT Edu Alexa Fluor 488 Flow Cytometry Assay Kit (LifeTechnologies, Saint Aubin, France, <https://www.thermofisher.com>) according to manufacturer’s instructions. Briefly, 18 hours prior to analysis, 20 μ M 5-ethynyl-2'-deoxyuridine (Edu), was added to the cell culture. Cells were then washed with PBS, fixed, permeabilized, labeled with an Alexa Fluor 488 azide and analyzed by flow cytometry. RNA synthesis was monitored using 5-Ethynyl-uridine (5-EU; Enzo life science, Villeurbanne, France, <http://www.enzolifesciences.com/>), following the same protocol, except that 5-EU was used at a final concentration of 400 μ M. For both DNA and RNA syntheses, the cells were concomitantly stained with HE to allow better discrimination. Protein synthesis was assessed using the Click-iT HPG Alexa Fluor

Protein synthesis assay kit (Life Technologies, Saint Aubin, France, <https://www.thermofisher.com>). For this purpose, the hMSCs were treated with L-homopropargylglycerine (HPG) in a methionine-free-media in either the presence or absence of 50 μ M cyclohexamide 1 hour prior to flow cytometry analysis.

Quantification of Viable and Apoptotic Cells

Viable hMSCs were identified after addition of both propidium iodide (PI; Sigma-Aldrich, St Quentin Fallavier, France, <http://sigmaaldrich.com>; at a final concentration of 0.5 μ g/ml) and HE (1 μ g/ml) at 37°C for 15 minutes. The labeled cells were first photographed using the Nikon Eclipse TE2000-U microscope, and then washed with PBS, trypsinized, and analyzed using flow cytometry. Cells which had been stained both HE positive and PI negative were identified as “viable cells,” whereas cells which had been stained both HE positive and PI positive were identified as “dead cells.” At each prescribed time point, cell viability was expressed as the number of viable cells normalized by the respective viable cell number at D0.

ATP/ADP Levels

Intracellular levels of both ATP and ADP were monitored using the ApoSENSOR ADP/ATP ratio assay kit (Enzo Life Science, Villeurbanne, France, <http://www.enzolifesciences.com/>) following the manufacturer's instructions. At the prescribed time points, the hMSCs were rinsed with PBS, trypsinized, and stored at -80°C until further analysis. Bioluminescence indicative of both the ATP and ADP levels was measured using a Veritas Microplate Luminometer (Turner BioSystems, Charbonnières-les-Bains, France, <https://france.promega.com>).

In Vivo Assessment of Cell Viability

The protocol had received approval by the Ethics Committee on Animal Research of Lariboisiere/Villemin (number CEEA-LV/2014-10-20) in Paris, France, and was carried out in accordance with the new European Directive 2010/63/EU on the protection of animals used for scientific purposes. Two models of implantation were used. In a “closed system,” cell-containing constructs were prepared by loading 2×10^5 of either SD-hMSCs-gluc(−) or UP-hMSC-gluc(+) in 200 μ l fibrin gel (18 mg/ml fibrinogen, Sigma-Aldrich, St Quentin Fallavier, France, <http://sigmaaldrich.com>; 0.72 U/ml Thrombin, Baxter, Guyancourt, France, <http://www.baxter.fr/>) in diffusion chambers (membrane filters with 0.45 μ m diameter pores; Millipore, Molsheim, France, <http://www.merckmillipore.com/FR>). One day after preparation, the cell-constructs were subcutaneously implanted in nude mice as previously described [7]. At the prescribed time points (D3, D7, and D14), the diffusion chamber constructs were explanted and the contained cells were collected by enzymatic digestion (using 10X Trypsin - 10mM EDTA for 15 minutes at 37°C). Cell viability was assessed by cytometry. For the “open system,” cell-containing gels were directly implanted in mice. hMSCs were previously genetically modified by their transduction with a lentiviral vector encoding firefly luciferase (pRRLsin-MND-Luc-IRES2-ZsGreen-WPRE; TRANSBIO MED; Bordeaux, France, <http://transbiomed.u-bordeaux2.fr/>) as previously described [7] and further expanded. Prior to implantation, 3×10^5 of either SD-hMSCs^{LUC} or UP-hMSCs^{LUC} were embedded within 300 μ l fibrin gel (18 mg/ml fibrinogen, Sigma-Aldrich, St Quentin Fallavier, France, <http://sigmaaldrich.com>; 0.72 U/ml Thrombin,

Baxter, Guyancourt, France, <http://www.baxter.fr/>) and cell-containing gels were subcutaneously implanted in nude mice. Cell viability in constructs was monitored noninvasively in vivo using a bioluminescence imaging system (Ivis, Lumina II, Caliper Life Sciences, Villebon-sur-Yvette, France, <http://www.perkinelmer.com/lab-solutions/>) as previously described [21] throughout the 21 days of implantation (D7, D14, D21). Results were expressed as a percentage of the bioluminescence signal measured on D0 ($n = 6$ constructs per group). To further assess the viability of implanted cells, cell-containing constructs ($n = 4$ constructs) were explanted after 7 days of implantation, fixed in 4% paraformaldehyde (pH 7.4) and embedded in paraffin. Sections were processed for human beta-2-microglobulin (h β 2-MG) (a membrane protein that enables tracking human cells) immunodetection, using the Kit Envision + (Dako, Les Ulis, France, <http://www.dako.com>) and the polyclonal rabbit anti-h β 2-MG (1/1,000; Novocastra, Nanterre, France, <http://www.leicabiosystems.com/ihc-ish-fish/immunohistochemistry-ihc-antibodies-novocastra-reagents/>) as primary antibody as previously described [7].

Cell Functionality upon Reperfusion

To assess the protein secretory potential of SD-hMSCs, these cells were cultured under ischemic conditions for 7 days, then reperfused with glucose (added to the supernatant for a final concentration at 5 g/l), and cultured under anoxia for 7 additional days; these cells were designated as SD-hMSCs-gluc(r). At the prescribed time, the supernatants were collected and their protein contents were determined and compared to those obtained from nonreperfused SD-hMSCs-gluc(−) and from UP-hMSCs-gluc(+) groups.

To assess the post-ischemic cell functionality after 14 days of culture under ischemia in vitro, SD-hMSCs-gluc(−) and UP-hMSC-gluc(+) were transferred back to normoxic (21% O₂) conditions and further cultured in α MEM containing 1 g/l of glucose and 10% FBS. To assess the osteogenic and adipogenic differentiation of reperfused SD-hMSC, the cells were trypsinized upon reaching confluence, re-seeded, and further cultured either in osteogenic medium (containing 10^{-7} M dexamethasone, 150 mM ascorbic acid-2 phosphate, and 2 mM beta glycerophosphate) or in adipogenic medium (containing 10^{-7} M dexamethasone, 0.5 mM IsoButylMethylXanthine, 60 μ M indomethacine, and 5 μ g/ml insulin; all chemicals from Sigma-Aldrich, St Quentin Fallavier, France, <http://sigmaaldrich.com>). In parallel, naïve hMSCs (i.e., unpreconditioned and not exposed to anoxia/ischemia) were seeded and cultured under similar conditions as controls. After 14 days of culture in osteogenic medium, alkaline phosphatase activity was determined both by staining the cell cultures in situ and by quantifying alkaline phosphatase activity in cell lysates as previously described [22]. After 28 days of culture in osteogenic medium, the presence of calcium-containing deposits in the extracellular matrix was detected using Alizarin Red stain, and visualized using light microscopy. After 21 days of culture in adipogenic medium, lipid accumulation was assessed by staining the cells using Oil Red O stain, and visualizing them using light microscopy.

To assess the cell proliferative function after either 0, 3, or 7 days of implantation in mice, cells were collected from explanted diffusion chambers after enzymatic digestion and seeded at 2,500 cells per cm² and further cultured under

standard culture conditions for 7 additional days. At day 4 and day 7, viable cells were quantified as described in “Quantification of viable and apoptotic cells” section.

Protein Expression

Both the intracellular protein content and the protein content in the cell culture supernatants were quantified using the Pierce BCA Protein Assay Kit (Thermo Scientific, Rockford, IL, <https://www.thermofisher.com>) according to the manufacturer’s instructions; bovine serum albumin (BSA) was used as the standard. Results were expressed as “protein content per cell” (ng per cell). Activation of mTOR was evaluated by analyzing the phosphorylation of its downstream effector target S6 kinase 1 (S6K1) [23]. Briefly, cells were lysed and analyzed by Western blotting using primary antibodies against Phospho-p70 S6 Kinase (Thr389; Cell Signaling Technology, Danvers, MA, <https://www.cellsignal.com>) [24].

Autophagic LC3B Immunofluorescence Detection

Analyses of autophagy were performed by the immunofluorescence detection of the endogenous LC3B-II protein. Cells were seeded at 10^4 cells per cm^2 onto glass coverslips and further cultured under prescribed cell culture conditions. Four hours prior to the analysis, the cells were either treated with 400 nM Bafilomycin (to block autophagosome degradation) or were left untreated. At D0, D1, and D3, cells were rinsed once with PBS, methanol-fixed, permeabilized and labeled with rabbit anti-LC3B polyclonal antibody (Sigma L7543, Sigma-Aldrich, St Quentin Fallavier, France, <http://sigmaaldrich.com>), followed by incubation with an anti-rabbit secondary antibody conjugated to a FluoProbes-488 (Interchim, Montluçon, France, <http://www.interchim.com/>) for visualization. Fluorescent photographs were taken using Axiovert 200M Fluorescence microscope (ZEISS, Marly le roi, France, http://www.zeiss.fr/corporate/fr_fr/home.html). The cells containing at least 5 LC3-positive punctae (autophagosomes) were counted and these numbers were normalized over the numbers (>200) of cells analyzed

Cellular Bioenergetic Measurements

The oxygen consumption rate (OCR) and the extra cellular acidification rate (ECAR) of the SD-hMSCs and UP-hMSCs were determined using a XF96^e Flux analyzer (Seahorse Bioscience XF96 Instrument, North Billerica, MA) and the method described in the literature [25]. Briefly, hMSCs were seeded at 14×10^3 and 8×10^3 cells per well for SD-hMSC and UP-hMSC groups, respectively, in XF96 cell culture plates at D-3. At D-2, the SD-hMSCs were preconditioned for 2 days as previously described. The “glycolysis stress test” was performed in XF base medium supplemented with 2 mM glutamine while the “mito stress test” was performed in XF base medium supplemented with 2 mM glutamine, 1 mM pyruvate and 10 mM glucose according to the manufacturer’s instructions. At the end of each one of these experiments, the cells on XF96 plates were fixed and the cell nuclei were stained using 1 $\mu\text{g}/\text{ml}$ HE for 30 minutes. The “average numbers” of cells present in at least 4 wells per group tested were counted in order to normalize OCR and ECAR expressed in “ $\text{pmol}/\text{min}/\text{cell}$ ” and “ $\text{mpH}/\text{min}/\text{cell}$ ”, respectively.

Glucose Metabolism Pathways Gene Expression

RT-qPCR targeting expression of 84 genes implicated in the human glucose metabolism was performed. Briefly, cells were rinsed with PBS, RNA were extracted using Trizol, collected, and kept at -80°C for further analyses. Reverse transcriptase was performed using 1.5 μg of purified RNA and the superscript II enzyme (LifeTechnologies, Saint Aubin, France, <https://www.thermofisher.com>); the cDNA thus obtained was used for Glucose Metabolism RT2 Profiler PCR Array (Qiagen, Venlo, Netherlands, <https://www.qiagen.com/fr/>) following the manufacturer instructions and using the MyiQ Single-Color Real-Time PCR Detection System (Biorad, Marnes-la-Coquette, France, www.bio-rad.com).

Glucose and Lactate Assays

Glucose and lactate concentrations were measured in the supernatants collected during the ischemic period, using a biomedical ARCHITECT C8000 (Abbott Diagnostic) robot. Intracellular glycogen and glucose content were measured using the Glycogen assay kit (Biovision, Mountain View, CA, www.biovision.com), following manufacturer instructions. Results were expressed as “endogenous glucose content” (pmol/cell).

Statistical Analyses

Each experiment was conducted in triplicate and repeated in, at least, two separate occasions. Numerical data were expressed as mean \pm standard deviation ($\pm\text{S.D.}$). Statistical analyses were conducted using the Statgraphics centurion version XV.2 (Statpoint Technologies, Inc, Warrenton, Virginia, <http://www.statgraphics.com>) software. The quantitative kinetics data were analyzed using two-way analysis of variance. The nonparametric Mann–Whitney *U* test was used to analyze data from two independent samples. For all analyses, differences at $p < .05$ were considered as statistically significant.

RESULTS

Quiescence Preconditioning by Serum Deprivation Leads to Reduced Anabolic hMSC Functions

SD for 48 hours led to a small, yet sizeable (24%), decrease in viable hMSC numbers (Fig. 1A). Both intracellular ATP and ADP levels of SD-preconditioned hMSC (SD-hMSC) were similar to those of unpreconditioned hMSC (UP-hMSCs) (with an ATP/ADP ratio of 7.6; Fig. 1B); the total protein content (Fig. 1C) of SD-hMSCs was similar to those of (UP-hMSCs) as well, indicating that SD-hMSCs were metabolically healthy.

SD-hMSCs stopped proliferating and most of them arrested in the G0/G1 phase, compared to UP-hMSCs (Fig. 1D). The fraction of SD-hMSCs that were not synthesizing DNA was significantly higher than that found in UP-hMSCs (Fig. 1E). In addition, RNA synthesis and, consequently, protein synthesis were both greatly reduced in SD-hMSCs (Fig. 1F, 1G). Taken together, these results demonstrated that SD-hMSCs shifted into a quiescent state.

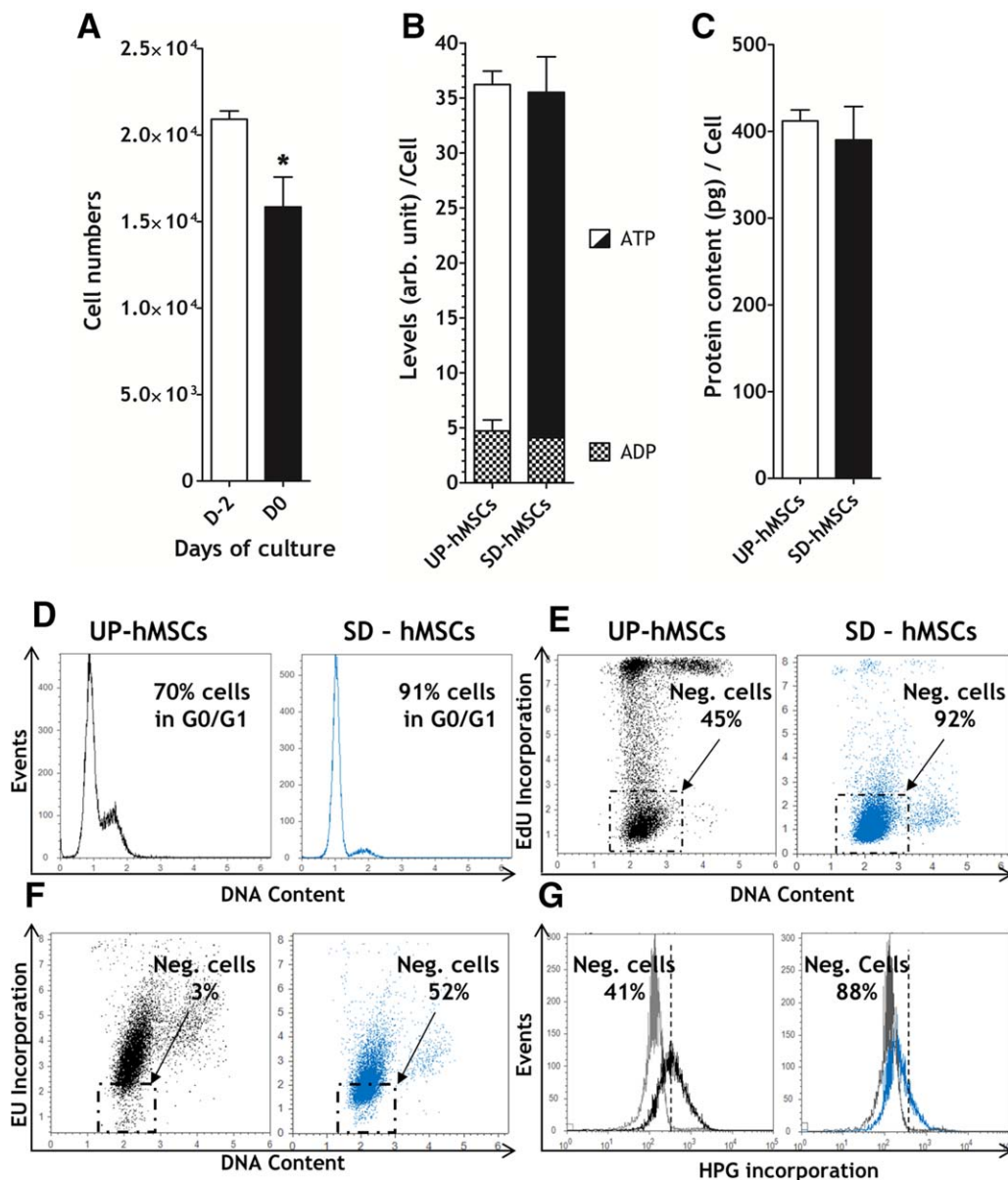


Figure 1. Quiescence preconditioning by serum deprivation (SD) leads hMSCs to cell cycle arrest and reduced anabolic functions. hMSCs were preconditioned by serum deprivation for 48 hours. **(A):** Quantification of viable cells stained with propidium iodide before (D-2) and after SD preconditioning (D0) ($n = 6$). **(B):** ATP and ADP levels per cell ($n = 3$) **(C)** and protein content per cell were measured for both SD-hMSCs and UP-hMSCs at D0 ($n = 6$) **(D)** Cell cycle distribution **(E)** DNA, **(F)** RNA and **(G)** protein syntheses of both SD-hMSCs and UP-hMSCs were analyzed by flow cytometry at D0. hMSCs incubated with cycloheximide (an inhibitor of protein synthesis) served as negative control (gray plot) ($n = 3$) **(G)**. Results are expressed as means \pm SD. *, p value $< .05$ versus (D-2) (Mann-Whitney test). Abbreviations: EU, 5-Ethynyl-uridine; hMSCs, human mesenchymal stem cells/multipotent stromal cells; HPG, L-homopropargylglycerine; SD-hMSCs, preconditioned cells; UP-hMSCs, Unpreconditioned hMSCs.

Quiescence Preconditioning Maintains Viability of hMSCs Which Remain Functional when Reperfused In Vitro

The benefit of quiescence preconditioning for SD-hMSC survival under ischemic conditions was evaluated. After 14 days of culture in either near-anoxia or ischemia, cell morphology was greatly impacted (Fig. 2A). While UP-hMSCs-gluc(+) spread out over time (Fig. 2Ac), UP-hMSCs-gluc(-) appeared dead, with ghost cells amongst cellular debris (Fig. 2Ad). In contrast, SD-hMSCs-gluc(-) exhibited few morphological changes (Fig. 2Ae) and remained similar to SD-hMSCs at D0 over the entire 14-day culture period.

Both UP-hMSCs-gluc(+) and SD-hMSCs-gluc(-) cultures contained few dead (PI positive) cells (Fig. 2Bb-2Bf). In contrast, most cells from the UP-hMSCs-gluc(-) group were PI positive (Fig. 2Bd). These results were confirmed by cell quantification (Fig. 2C). The number of viable cells decreased as early as D3 for the three groups tested. At D3, only one third of UP-hMSCs-gluc(-) were still alive while two third of both SD-hMSCs-gluc(-) and the UP-hMSCs-gluc(+) cells were viable (Fig. 2C). Viability of the UP-hMSCs-gluc(-) cells decreased as a function of time; all cells were dead at D10 (Fig. 2C). In the presence of glucose, however, the UP-hMSCs-gluc(+) cells maintained their viability over the culture period

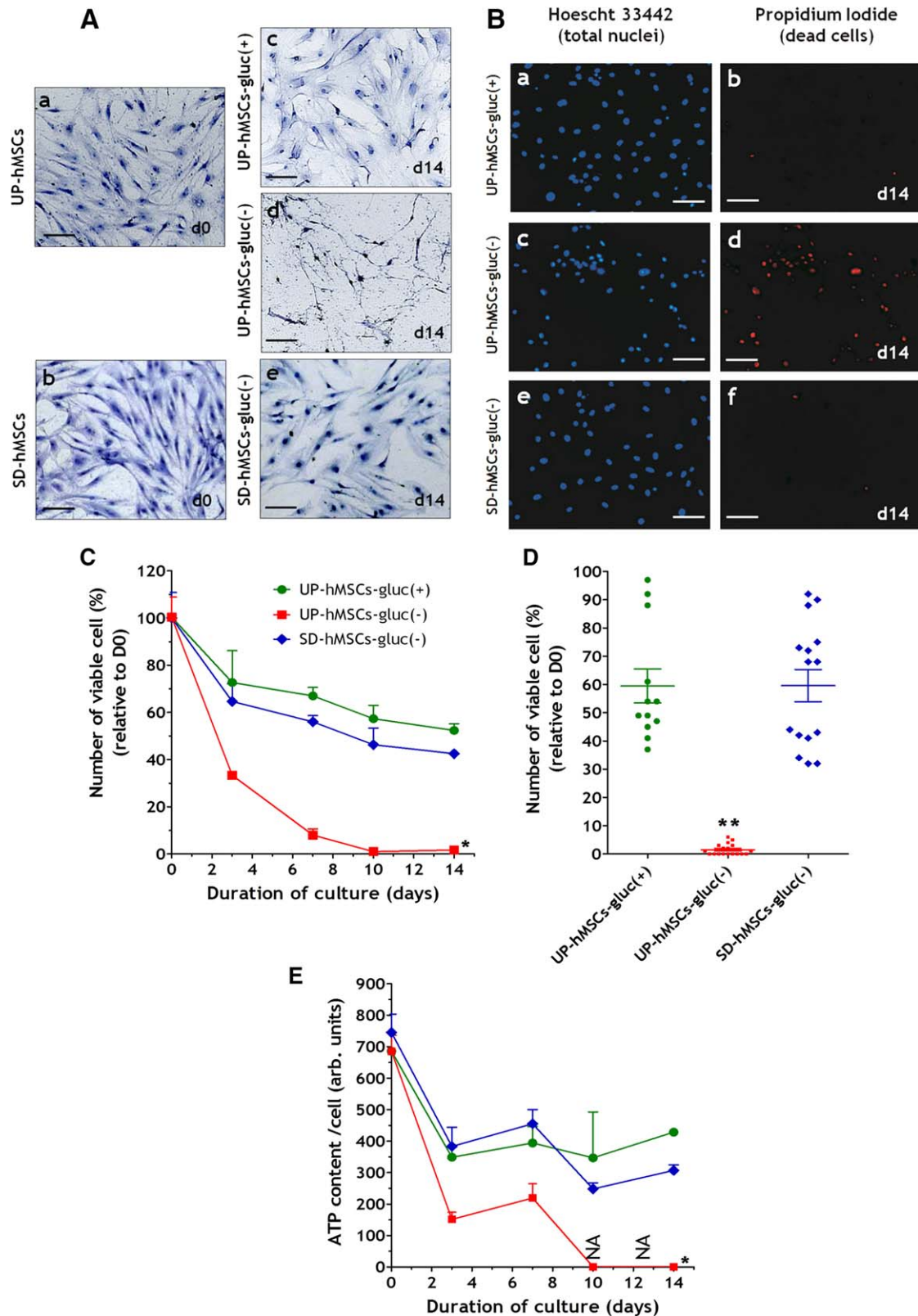


Figure 2. Quiescent SD-hMSCs maintain both viability and ATP content when cultured under ischemia in vitro. **(A)**: Representative images of Hematoxylin and Eosin staining of UP-hMSCs **(Aa)**, SD-hMSCs **(Ab)** at D0, and, UP-hMSCs-gluc(+) **(Ac)**, UP-hMSCs-gluc(-) **(Ad)**, and SD-hMSCs-gluc(-) **(Ae)** after 14 days of culture under anoxia/ischemia ($n = 3$) **(B)**: Representative images of Hoescht 33442- (total nuclei) and propidium iodide- (dead cells) stained hMSCs at D14 ($n = 3$) **(C)**: Cell viability in UP-hMSCs-gluc(-), UP-hMSCs-gluc(+) and SD-hMSCs-gluc(-) cell groups assessed after HE and PI staining and analyzed by flow cytometry. **(C)**: Time-course of cell viability assessed during the ischemic period. One experiment ($n = 3$) representative of five carried out. **(D)**: Dot plot for cell viability values ($n = 15$) obtained from 5 independent experiments after 14 days of culture under anoxia/ischemia. **(E)**: Time-course of ATP content per cell assessed during the ischemic period ($n = 3$). Results are expressed as means \pm S.D. *, $p < .05$ versus UP-hMSCs-gluc(+) (Two-way ANOVA), **, p value $< .0001$ versus UP-hMSCs-gluc(+) (Student's t test). Abbreviations: hMSCs, human mesenchymal stem cells/multipotent stromal cells; NA, not applicable; SD-hMSCs, preconditioned cells; UP-hMSCs, Unpreconditioned hMSCs.

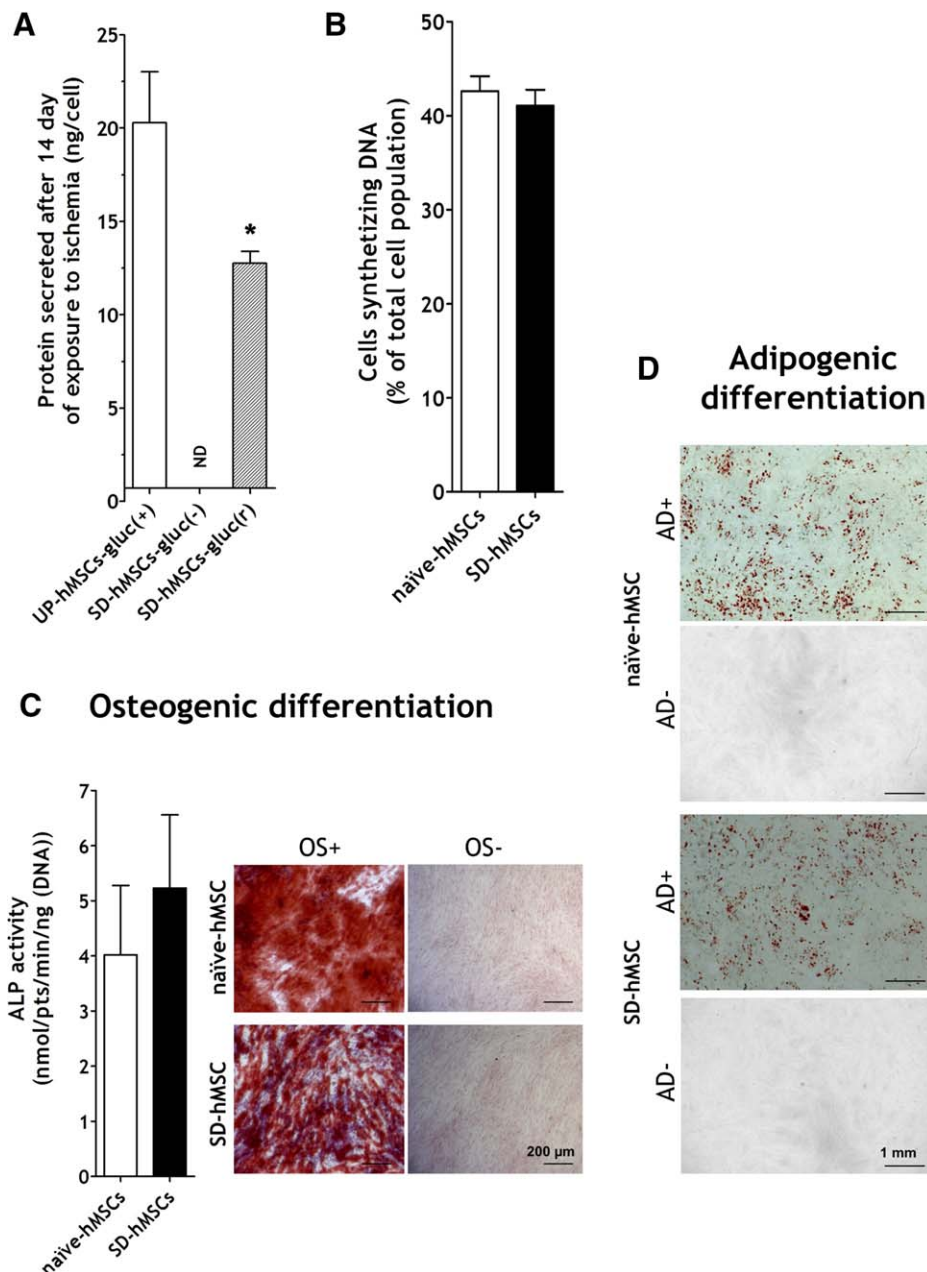


Figure 3. Reperused SD-hMSCs remain functional after sustaining 14 days of ischemia. **(A):** After 14 days of culture under anoxic/ischemic conditions, supernatants were collected and their protein content was assessed for both UP-hMSCs-gluc(+) and SD-hMSCs-gluc(-). Supernatant protein content of SD-hMSCs reperused with glucose on the 7th day of exposure to ischemia (SD-hMSCs-gluc(r)) was also evaluated ($n = 3$). **(B):** The proliferative potential of SD-hMSCs exposed to ischemia for 14 days and reperused (10% FBS, 21% O_2 , 1g/l glucose) for 48 hours was evaluated by DNA synthesis analysis ($n = 3$). **(C, D):** After reperfusion, differentiation potential of SD-hMSCs was evaluated in comparison with naïve-hMSCs. **(C):** ALP expressed by reperused hMSCs cultured in osteogenic media for 14 days ($n = 3$); Alizarin Red (calcium accumulation in the extracellular matrix) stainings of reperused hMSCs after 28 days of culture in either osteogenic media (OS+) or standard media (OS-)(α MEM +10% FBS) ($n = 3$). **(D):** Oil red O stainings of reperused hMSCs in either adipogenic media (AD+) or standard media (AD-)(α MEM +10% FBS) for 21 days ($n = 3$). Results are expressed as means \pm S.D. *, p value $< .05$ versus UP-hMSCs-gluc(+)(Mann-Whitney). Abbreviations: ALP, alkaline phosphatase activity, ND, Not detected; SD-hMSCs, preconditioned cells; UP-hMSCs, Unpreconditioned hMSCs.

with a survival rate of $59 \pm 21\%$ at D14 (Fig. 2D). Importantly, SD-hMSCs-gluc(-) exhibited a statistically similar survival rate as UP-hMSCs-gluc(+) with a survival rate of $60 \pm 22\%$ at D14 (Fig. 2D).

The bioenergetic status of hMSCs in each group was investigated during culture under ischemia/anoxia (Fig. 2E). Similar to the observed trends of the cell survival rates, UP-hMSCs-

gluc(+) and the SD-hMSCs-gluc(-) were the only two cell groups that maintained significant ATP levels over time. The ATP per cell content in these groups rapidly decreased, specifically by 50% at D3 compared to results obtained on D0, and was sustained over the 14-day period of cell culture. In contrast, the ATP content in UP-hMSCs-gluc(-) had already been decreased by 78% at D3 and was only detectable until D7. Concomitantly,

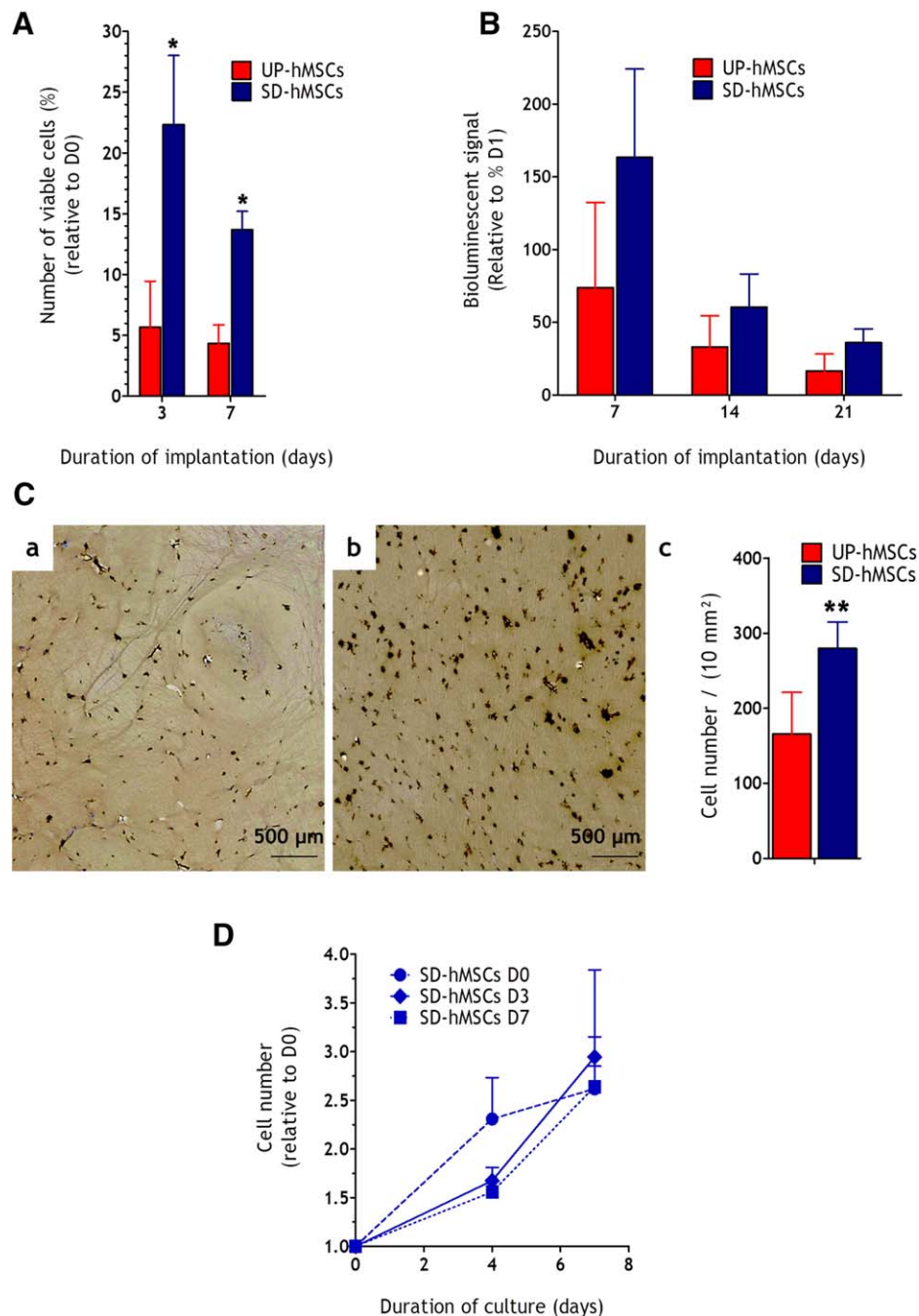


Figure 4. Quiescence preconditioning enhances viability of implanted hMSCs at early time post-implantation. **(A):** In vivo viability of either UP-hMSCs or SD-hMSCs assessed in a closed system. Cells embedded within a fibrin gel were loaded in a diffusion chamber and subcutaneously implanted in mice. The numbers of viable cells from explanted chambers were quantified by flow cytometry after the fibrin gel degradation. ($n = 3$). **(B):** In vivo cell viability assessed in an open system (in the absence of diffusion chamber). Bioluminescent signals from either viable SD-hMSCs^{Luc} or UP-hMSC^{Luc} cells loaded in a fibrin gel over the 21 days period of ectopic implantation in nude mice ($n = 6$). **(C):** Anti-h β 2-MG immunostaining on cell-constructs containing either UP-hMSCs (Frame Ca) or SD-hMSCs (Frame Cb) after 7 days of ectopic implantation in nude mice. Numbers of h β 2-MG-positive cells detected per section (Frame Cc). Two stained sections from each construct were examined; ($n = 4$ constructs per group). **(D):** In vitro cell proliferation of SD-hMSCs extracted from constructs either nonimplanted (D0) or explanted at D3 and D7 days post-implantation ($n = 3$). Results are expressed as means \pm S.D. *, $p < .001$ versus UP-hMSCs (Two-way ANOVA followed by Bonferroni's post hoc test) **, p value $< .05$ (Mann-Whitney test). Abbreviations: SD-hMSCs, preconditioned cells; UP-hMSCs, Unpreconditioned hMSCs.

ADP levels were also diminished for all cell groups when these cells were exposed to ischemia for 14 days (data not shown).

The secretory potentials of UP-hMSCs-gluc(+) and SD-hMSCs-gluc(-) were determined at the end of cell

exposure to the anoxic/ischemic conditions (Fig. 3A). The amount of secreted proteins by SD-hMSCs-gluc(-) was undetectable in contrast to the high amount of secreted proteins by UP-hMSCs-gluc(+). Upon reperfusion, however,

the secretory potential SD-hMSCs-gluc(r)) was partially restored, up to 60% compared to the UP-hMSCs-gluc(+) group.

The proliferative ability and differentiation potential of SD-hMSCs reperfused under standard cell culture conditions were compared to those of fresh naïve-hMSCs. The rate of SD-hMSCs synthesizing DNA was similar to that obtained for naïve-hMSCs 48h postreperfusion (Fig. 3B). The ALP activity and matrix mineralization (which represent early and late markers of osteogenic differentiation, respectively) in reperfused SD-hMSC cell cultures were both similar to the ones determined for naïve-hMSCs (Fig. 3C). In addition, similar amounts of stained lipid droplets (a marker for adipogenic differentiation), were observed in both the reperfused SD-hMSCs and naïve-hMSCs (Fig. 3D).

Quiescence Preconditioning Enhances Viability of Implanted hMSCs In Vivo

To confirm these outcomes in vivo, two models of implantation were used. First, in a closed system, cells were embedded within a fibrin gel then further loaded in a diffusion chamber (a model that prevents infiltration of host cells and mimics a highly ischemic environment) and subcutaneously implanted in mice. Quantification of viable cells showed that the viability of both cell groups dramatically decreased over time. However, the cell numbers of SD-hMSCs were significantly higher as compared to UP-hMSCs at both day 3 and 7 (4- and 3-fold, respectively; $p < .001$) (Fig. 4A); then, the SD-hMSC group reached a same death rate as control group at day 14 postimplantation (data not shown).

Second, in an open system reflecting an in vivo model for engineered tissue regeneration, both SD-hMSCs^{Luc} and UP-hMSCs^{Luc} were loaded within a fibrin gel and subcutaneously implanted in nude mice. The bioluminescence signal from both cell groups decreased over time indicating the disappearance of the implanted cells over the 21 days period of implantation (Fig. 4B). At each time points tested, the bioluminescence signal from SD-hMSCs^{Luc} was higher although not significantly different than the one from UP-hMSCs^{Luc}. To validate this trend, the numbers of hβ2-MG-positive cells were counted on histological sections from cell-constructs explanted at day 7 postimplantation. Results showed a significant enhanced (1.7-fold; $p < .05$) number of hβ2-MG-positive cells in the SD-hMSC group compared to the UP-hMSC group (control group) (Fig. 4C). At this time point, however, the number of apoptotic cells (TUNEL-positive cells) across the sections remained low (<10%) for both cell groups (data not shown). In order to evaluate whether surviving SD-hMSCs in cell-constructs could be re-awakened upon reperfusion, cells from construct explanted after 3, and 7 days post-implantation were recovered and cultured under standard in vitro tissue culture conditions and compared to nonimplanted cells (Day 0). The proliferation rates of reperfused cells were comparable in all SD-hMSC groups tested (Fig. 4D). Altogether, these data provided evidence that SD-hMSCs showed enhanced survival in vivo at early time (7 days) postimplantation in mice and surviving cells remained functional.

Quiescent Preconditioned hMSCs Adopt a Metabolic Profile Suitable for Withstanding Metabolic Stress

We next sought to determine the underlying mechanism for the beneficial effect of the quiescence preconditioning on cell

survival during ischemia. The responses of energy-sensing pathways in SD-hMSCs (compared to UP-hMSCs) were examined. AMPK, which is one of the central regulators of cellular and organismal metabolism was not modified (data not shown). By contrast, compared to UP-hMSCs, SD-hMSCs exhibited the suppression of the phosphorylation of S6K (Fig. 5A), a downstream target of mTORC1. Such suppression was maintained when SD-hMSCs were cultured in ischemia. In addition, UP-hMSCs cultured in either ischemia or anoxia exhibited suppression of pS6K phosphorylation (Fig. 5A).

Since mTORC1 is known to control autophagy, the impact of quiescence preconditioning on autophagy was examined (Fig. 5B, 5C). At D0, the percentage of cells containing LC3-positive (a marker of autophagosomes) punctae significantly increased upon quiescence preconditioning (38% in UP-hMSC vs. 68% in SD-hMSC; Fig. 5C). Addition of bafilomycin showed that the autophagic fluxes were increased in both groups (Fig. 5Bb-5Bd). After one day (D1) under anoxia/ischemia, both autophagic basal activities and autophagic flux increased (85%-95%) in the three cell groups tested (Fig. 5Be-5Bj). In contrast, the autophagic activities slightly decreased at D3 for the three treatment groups (Fig. 5C). Addition of bafilomycin revealed that UP-hMSCs-gluc(-) reduced their autophagic flux whereas UP-hMSCs-gluc(+) and SD-hMSCs-gluc(-) maintained their autophagic fluxes (Fig. 5Bk-5Bp, 5C). Addition of 3-methyladenine (3MA), an inhibitor of autophagic/lysosomal protein degradation to SD-hMSCs resulted in a significant decrease in SD-hMSC survival rate during the 14 days of culture under ischemia (specifically, by 11% at day 3 and by 34% at day 14; Fig. 5D).

To gain further insights into what distinguishes SD-hMSCs from UP-hMSCs, we analyzed their bioenergetic profiles before exposure to ischemia/anoxia. Their mitochondrial oxygen consumption rates (OCR) and extra cellular acidification rates (ECAR) were monitored using an extracellular flux analyzer. The mitochondrial stress test indicated that SD-hMSCs displayed lower basal (before addition of oligomycin) and maximal (after addition of the FCCP mitochondrial uncoupler) respiratory capacities, as well as a lower minimal respiratory reserve, than UP-hMSCs (Fig. 6A). The glycolytic stress test (Fig. 6B) indicated a sudden increase of lactate production in the presence of glucose, providing evidence that SD-hMSCs have a higher glycolytic capability than UP-hMSCs. Blocking respiration (using oligomycin) did not increase the ECAR of SD-hMSCs, indicating that these cells do not possess any glycolytic reserve (Fig. 6B).

A complete analysis of the gene expression profiles of metabolic enzyme transcripts in both SD-hMSCs and UP-hMSCs at D0 as well as their counterparts under either anoxia or ischemia at D3 was performed. Cluster analysis of all genes tested showed that the enzyme profiles in SD-hMSCs and UP-hMSCs under normoxia were more similar to each other than to the other treatment groups, suggesting that oxygen deprivation causes the greatest metabolic change in hMSCs (Supporting Information 2A). This observation was confirmed by both glycolysis and TCA cluster analyses. Under ischemia/anoxia, most of the glycolysis-regulating enzymes in SD-hMSCs-gluc(-), UP-hMSCs-gluc(+) and UP-hMSCs-gluc(-) were upregulated (specifically, on average 3.4-, 3.0- and 4.4-fold increase, respectively; Supporting Information 2B) while TCA-regulating enzymes were downregulated (from 1.5- to

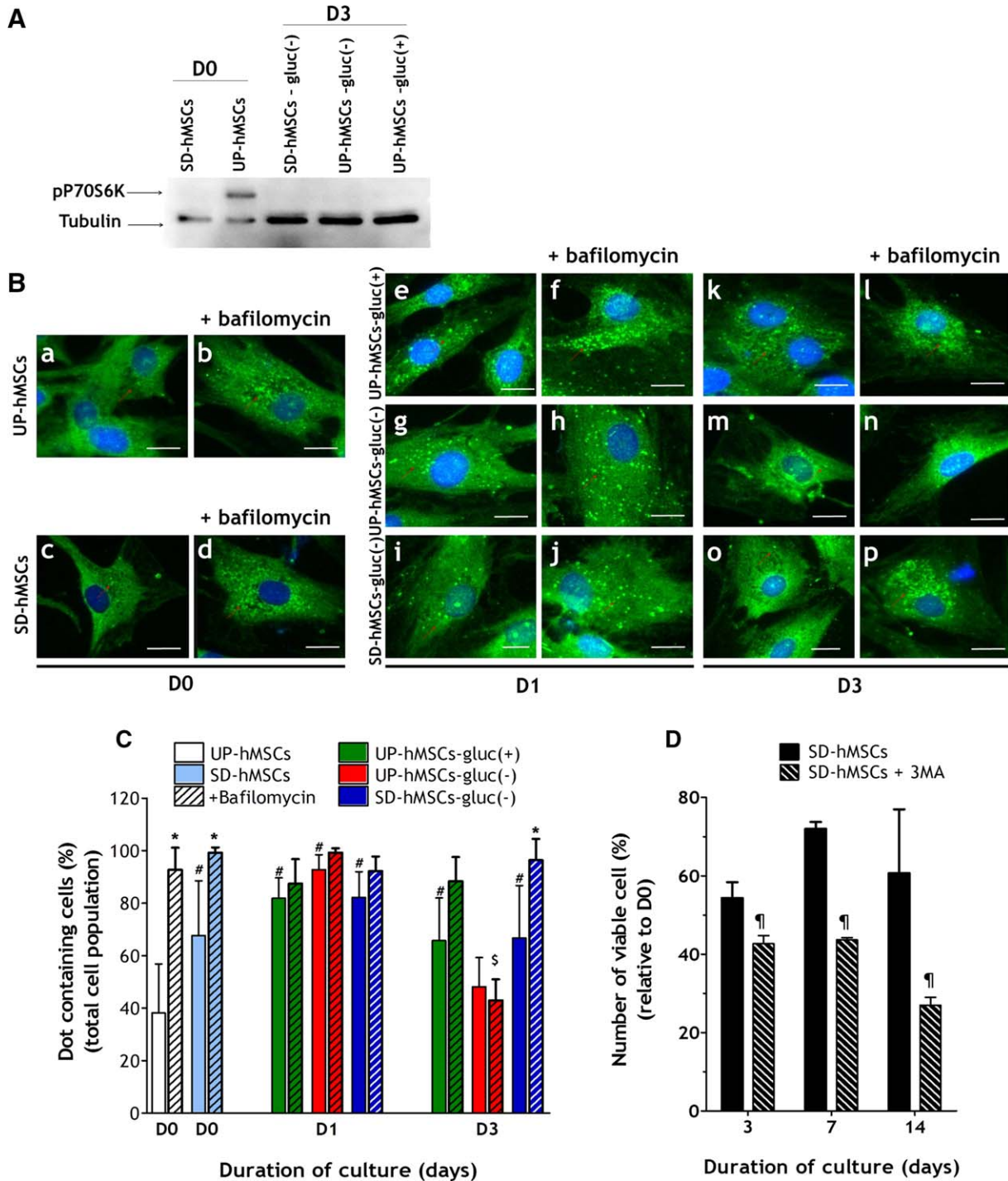


Figure 5. Quiescent SD-hMSCs inhibit mTORC1 and activate autophagy. **(A):** Representative immunoblot of phospho-p70 S Kinase (pP70S6K, a downstream effector of the activated mTOR) in SD-hMSCs and UP-hMSCs either at D0 or after 3 days under anoxia/ischemia. Tubulin was used as the reference protein for normalization ($n = 2$). **(B, C):** Autophagic activity in both SD-hMSCs and UP-hMSCs before (D0) and during the ischemic/anoxic episode. Addition of bafilomycin 4 hours prior the analysis enables to assess the autophagic flux (autophagosome accumulation). **(B):** Anti-LC3 immunofluorescence analysis of autophagosomes (green dot-like structures) in UP-hMSCs or SD-hMSCs at D0 (**a-d**), D1 (**e-j**), and D3 (**k-p**). **(C):** Quantification of cells containing at least 5 LC3-positive punctae normalized over a minimum of 200 cells analyzed. **(D):** Cell viability of SD-hMSCs cultured under ischemia in the presence of 3MA, an inhibitor of autophagic/lysosomal protein degradation ($n = 3$). Results are expressed as means \pm S.D. *, $p < .05$ for each cell group with bafilomycin versus cell group w/o bafilomycin (Mann-Whitney); #, $p < .05$ for each cell group w/o bafilomycin versus UP-hMSCs (at D0) (Mann-Whitney); §, $p < .05$ for cell group with bafilomycin versus to UP-hMSCs-gluc(+) with bafilomycin (Mann-Whitney). ¶, $p < .05$ versus SD-hMSCs (Two-way ANOVA followed by Bonferroni's post hoc test). Abbreviations: hMSCs, human mesenchymal stem cells/multipotent stromal cells; SD-hMSCs, preconditioned cells; UP-hMSCs, Unpreconditioned hMSCs.

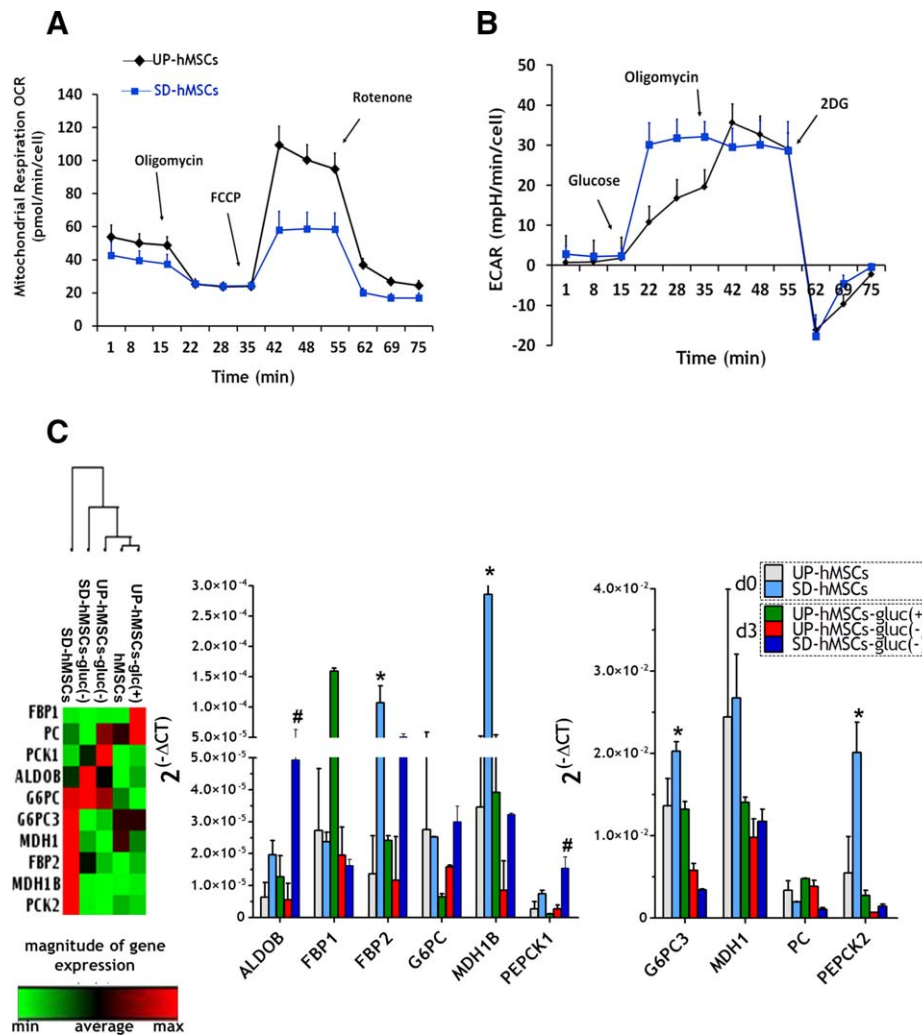


Figure 6. Quiescent SD-hMSCs adopt a metabolic profile suitable for withstanding metabolic stress. **(A, B)** Mitochondrial oxygen consumption rates (OCR) and extra cellular acidification rates (ECAR) in UP-hMSCs or SD-hMSCs monitored using the Seahorse XF96e Flux analyzer. **(A):** OCR when cells were cultured in XF base medium supplemented with 2 mM glutamine, 1mM pyruvate and 10mM glucose, and exposed to oligomycin (Oligo) at 15 minutes, FCCP at 35 minutes and rotenone at 55 minutes ($n = 4$). **(B):** ECAR when cells were cultured in the XF base medium supplemented with 2 mM glutamine and exposed to glucose (Gluc) at 15 minutes, oligomycin at 35 minutes and 2DG at 55 minutes. Results are expressed as means \pm S.D. ($n = 4$). **(C):** Gluconeogenesis pathway-related gene expression in both SD-hMSCs and UP-hMSCs at D0 as well as their counterparts under either anoxia or ischemia at D3. Gene expressions, normalized by the house-keeping genes expression of Beta-2-Microglobulin, Ribosomal Protein L13a and Beta-actin, are presented using the heat map representation and cluster analysis (with elevated expression shown in red and decreased expression in green; left panel). Expression levels are presented in $2^{(-\Delta CT)}$ format (right panel). Values represent means \pm S.D. ($n = 2$). *, $p < .05$ versus UP-hMSCs at D0. #, $p < .05$ versus UP-hMSCs-Gluc(-) at D3 (ANOVA with Bonferroni's post hoc test). Abbreviations: 2DG, 2-Deoxy-D-glucose; ALDOB, Aldolase B; FBP1, FBP2, fructose-1,6-bisphosphatase 1 and 2; G6PC, G6PC3, glucose-6-phosphatase catalytic subunit; hMSCs, human mesenchymal stem cells/multipotent stromal cells; MDH1, MDH1B, malate dehydrogenase soluble; PC, pyruvate carboxylase; PEPCK1, PEPCK2, phosphoenolpyruvate carboxykinase 1 and 2; SD-hMSCs, preconditioned cells; UP-hMSCs, unpreconditioned hMSCs.

2.3-fold; Supporting Information 2C). Of note, when taking into account all genes tested under anoxia/ischemia, the profile of SD-hMSCs-gluc(-) was closer to the positive control group (UP-hMSCs-gluc(+)) than the negative control group (UP-hMSCs-gluc(-)) (Supporting Information 2A).

When comparing the SD-hMSCs and UP-hMSCs profiles at D0, the gluconeogenic enzyme group was the only one that was significantly (3.1-fold induction on average in SD-hMSCs relative to UP-hMSCs at D0; $p < .05$) enriched in upregulated genes (Fig. 6C). In particular, PEPCK1, PEPCK2 (phosphoenolpyruvate carboxykinases) and FBP2 (fructose-1,6-bisphosphatase isozyme 2), the key, nonreversible, enzymes were upregulated by 2.7- (although not significantly different), 3.7-

($p < .05$) and 7.8-fold ($p < .05$), respectively. Interestingly, under same ischemic conditions, the gluconeogenic enzymes in SD-hMSCs-gluc(-) remained upregulated (3.3-fold induction on average relative to UP-hMSC-gluc(-)) (Fig. 6C). Taken together, these data indicated that quiescence preconditioning inhibits mTOR, stimulates autophagy, and promotes a change of the energy-metabolic profile toward glycolysis accompanied by the expression of gluconeogenic enzymes.

Quiescent Preconditioned hMSCs use Alternative Pathways for Surviving Under Ischemia

The bioenergetic basis of SD-hMSC survival under ischemic conditions was compared to that of UP-hMSC controls. To

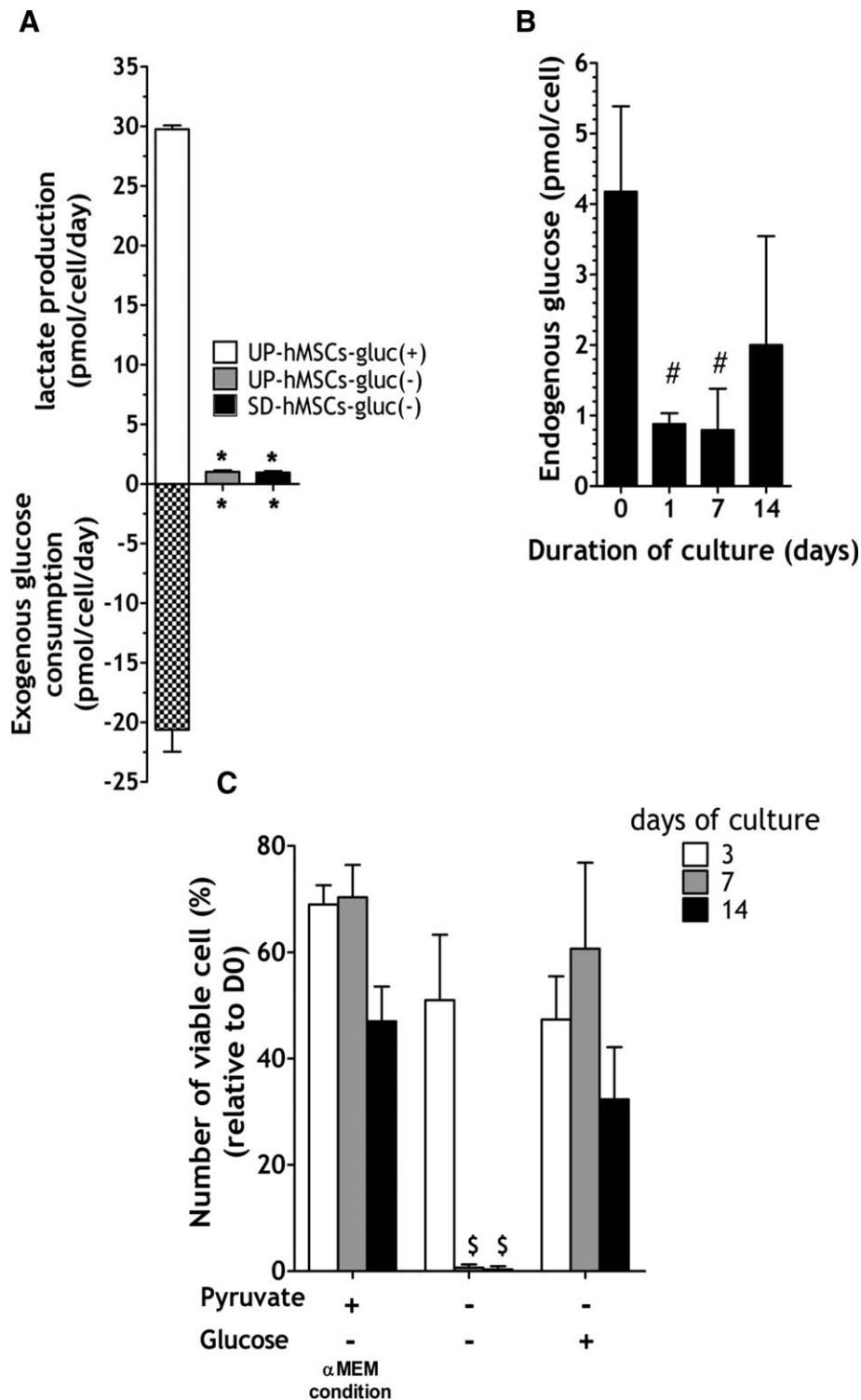


Figure 7. Quiescent SD-hMSCs use alternative metabolic fuel to survive under ischemia. **(A):** Lactate production and glucose consumption in SD-hMSCs-gluc(-) cultured under ischemic conditions for 14 days ($n = 3$). **(B):** Time-course of endogenous glucose content (including both intracellular glycogen and glucose contents) in SD-hMSCs-gluc(-) ($n = 3$). **(C):** Cell viability when SD-hMSCs when cultured in pyruvate- and/or glucose-free Dulbecco’s modified Eagle Medium under anoxia ($n = 3$). Results are expressed as means \pm S.D., *, $p < .05$ versus UP-hMSCs-Gluc(+) (Mann–Whitney); #, $p < .05$ for each time point versus D0 (Mann–Whitney); \$, $p < .05$ for each culture condition versus α MEM condition (Mann–Whitney). Abbreviations: α MEM, Alpha Minimum Essential Medium; hMSCs, human mesenchymal stem cells/multipotent stromal cells; SD-hMSCs, preconditioned cells; UP-hMSCs, unpreconditioned hMSCs

gain further insight into the mechanisms of ATP supply, glucose consumption and lactate production were analyzed in the three tested cell groups during the 14 days of cell culture under ischemic/anoxic conditions (Fig. 7A). Glucose consumption was 21 pmol/cell per day accompanied by a 30 pmol/cell per day lactate production for UP-hMSCs-gluc(+). Due to the lack of exogenous glucose in the cell culture media, SD-hMSCs-gluc(-) and UP-hMSCs-gluc(-) produced negligible lactate amounts over the 14 days of cell culture under ischemic conditions (Fig. 7A). These results confirmed that the UP-hMSCs-gluc(+) maintained their ATP level under near-anoxia by relying on exogenous glucose whereas the SD-hMSCs-gluc(-) maintained their ATP level in the absence of exogenous glucose and relied on other metabolic fuels for energy supply. The amount of endogenous glucose in SD-hMSCs indicated that these cells had a limited glucose stock (~4 pmol per cell) at D0 that decreased by 70%-80% as early as D1 post-ischemia although maintained such minimal content over the 14-day culture period (Fig. 7B).

In order to identify another potential metabolic fuel for SD-hMSCs under ischemic conditions, the role of pyruvate (present in the culture media used) on SD-hMSC survival was evaluated (Fig. 7C). Pyruvate withdrawal resulted in death of the entire cell population after 7 days of exposure to ischemia. When the supernatant culture media were supplemented with glucose, the SD-hMSCs survived throughout the 14 day-period of exposure to ischemia even in the absence of pyruvate (Fig. 7C). Taken together, these results indicated that hMSCs may rely on different nutrients available in the supernatant (glucose or pyruvate) to maintain their ATP levels and survive during anoxia.

DISCUSSION

In the present study, we considered an untapped preconditioning approach for improving hMSCs cell survival posttransplantation. We provided evidence, for the first time to our knowledge, that driving hMSCs into a quiescence state allows them to adopt a metabolic profile favorable to withstand exposure to severe, continuous, near-anoxia and total glucose depletion for up to 14 consecutive days *in vitro* and, most importantly, to improve their viability when implanted in an ischemic environment *in vivo*.

Cell quiescence can be induced either by mitogen deprivation, contact inhibition or disruption of cell-substrate adhesion [26, 27]. In this study, a protocol of preconditioning hMSCs by serum-deprivation for 48 hours proved effective in inducing hMSC quiescence. Such an approach could be the most appropriate strategy for future cell-based therapies as it is safe, easy-to-implement and does not require large cell numbers.

Anoxia, combined with serum- and glucose-deprivation, was chosen as the *in vitro* condition mimicking the *in vivo* ischemic metabolic environment found in large defects and was used to investigate the biological responses of hMSCs in that milieu [18, 28, 29]. As demonstrated in a previous report by our group [17], unpreconditioned hMSCs cultured under near anoxia (0.1% O₂) in the absence of glucose (ischemic conditions) died within 14 days of culture; in contrast, these cells remained viable in the presence of supplemented exogenous glucose. A key observation of the present study,

however, is that preconditioned, quiescent hMSCs cultured under ischemic conditions functioned similarly as hMSCs cultured under near anoxia in the presence of exogenous glucose *in vitro*: these cells remained viable and maintained their ATP level during the 14 day-period of the experiment. With the aim of deciphering the *in vivo* influence of quiescent preconditioning, hMSCs were then placed either in a closed system or in an open system and their survival rate assessed. Whereas the closed system, which prevents cell infiltration and reduces nutrient and oxygen supply, is intended to simulate the highly ischemic environment faced by hMSCs at the core of the implant, the open system, which allows host cell infiltration and implant revascularization, aims at mimicking the environment faced by hMSCs at the implant periphery. First, quiescent hMSCs implanted in the closed system exhibited a 4- and 3-fold significant increase in survival rate when compared to unpreconditioned cells at day 3 and 7, respectively. Nevertheless, the closed system model appeared stringent since control (unpreconditioned) hMSCs died within 3 days and quiescent hMSCs failed to survive at day 14. Additional studies are needed to thoroughly elucidate the mechanisms underlying the stringency of the response observed in this model. Second, when loaded in an open system, the rate of transplanted unpreconditioned hMSCs loss was slower and cells died within the 3-4 weeks postimplantation. These observations are in agreement with those reported by other groups and ours [3, 30, 31]. Most importantly, the number of h β 2-MG-positive quiescent preconditioned hMSCs was significant enhanced compared to the one of unpreconditioned hMSCs at day 7 postimplantation. The collective findings from both the *in vitro* and *in vivo* studies demonstrate that the viability of quiescent preconditioned hMSCs is enhanced during, at least, the first week postimplantation. This outcome could be beneficial for tissue engineering applications, since previous reports evidenced that enhanced viability (using a genetic HIF-1 α stabilization strategy) at early time resulted in improved regenerated bone tissue [32]. Among the various preconditioning strategies reported in the literature for enhancing the survival of progenitor cells, most of them rely on hypoxic preconditioning; interestingly, recent publications showed that such hypoxic preconditioning enhances cell survival by adaptation of the cell metabolism [30, 32]. Combining both quiescence and hypoxic preconditioning approaches could possibly have synergistic effects on cell viability but need further experimental assessments.

Another important observation is that the quiescent preconditioned hMSCs maintained both their proliferation (which was also observed for explanted cells) and secretory functions, as well as their potential for osteogenic and adipogenic differentiation upon reperfusion *in vitro*. The reperfusion conditions used here mimic an *in vivo* situation when a newly-formed vascular network has started invading the implanted TE cell construct. These results highlight the remarkable resilience of hMSCs with regard to ischemic insults and their capability to maintain progenitor cell properties.

Several studies reported that the quiescent state protects various types of cells (ranging from unicellular to complex multicellular organisms) from death under unfavorable environments [33, 34]. It is now recognized that quiescence of stem cells in their biological niche is critical for preserving their key functions. Attention also focused on the properties of quiescent

stem cells which allow them to withstand metabolic stress and to preserve genomic integrity over their lifetime [19, 35]. It should be noted that, cell quiescence even contributes to the maintenance of the viability and regenerative capability of cadaveric muscle stem cells *post mortem* [36]. Altogether, these studies indicate that the reduced metabolic activity of stem cells in the quiescent state plays a key role in the maintenance of both their survival and biologic functions.

Quiescence is characterized by a reversible arrest of cell proliferation and profound reduction of metabolic rate [34, 35]. In this study, most (90%) of SD-hMSCs were arrested in the G0/G1 phase of the cell cycle and exhibited reduced ATP-consuming anabolic functions such as nucleotide and protein syntheses. The fact that these resting cells maintained their intracellular ATP and protein contents, indicates that they had redirected their energy metabolism from nonessential and high-demanding energy anabolic processes toward essential "housekeeping" functions [37, 38]. The reduced observed anabolic functions of SD-hMSCs were associated with important changes in their energy metabolic profile. Entry into quiescence modulated energy-sensing pathways of cells such as mTOR, which is a master regulator of protein translation and proliferation [39, 40]. SD-hMSCs suppressed the mTOR kinase activity. The inhibition of mTOR signaling is known to promote autophagy [40]. The autophagic process is involved in survival responses of various cell types [41, 42], especially in cells in the quiescent state as a means to support basic cell functions. In this study, quiescence preconditioning stimulated autophagy in hMSCs *in vitro*. Moreover, SD-hMSCs maintained a high, and steady, autophagic activity in at least the early period exposure to ischemia *in vitro* and half of them died when autophagy was inhibited. These results indicated that the enhanced survival of SD-hMSCs under ischemic conditions *in vitro* was partly, but not only, due to the protective autophagy process.

Another important feature of the metabolic conversion resulting from quiescence preconditioning is that, despite adequate oxygen to support complete oxidation of glucose, SD-hMSCs displayed a shift of their energy metabolism from oxidative phosphorylation (OXPHOS) to glycolysis. Many stem cell types, including hematopoietic stem cells and hMSCs, which reside in hypoxic biologic niches, heavily rely on anaerobic glycolysis for their energy supply [43, 44]. A switch from OXPHOS to glycolysis was observed during conversion of somatic differentiated cells into induced pluripotent stem cells [45]. Therefore, dominant glycolytic metabolism of stem cells appears to be a hallmark of "stemness" that SD-hMSCs adopt upon quiescence preconditioning.

In this study, however, no upregulation of the glycolytic enzymes in SD-hMSCs compared to UP-hMSCs was observed. Under ischemia/anoxia, the glycolytic enzymes were upregulated while TCA-related enzymes were downregulated in both SD- and UP-hMSCs indicating that the glycolytic shift is more pronounced in the absence of oxygen. Interestingly, some gluconeogenic enzymes, in particular the key enzymes PEPCK-1 and PEPCK-2 (which convert oxaloacetate [OAA] to phosphoenolpyruvate [PEP]), were upregulated upon quiescence preconditioning. Although expression of these enzymes decreased under ischemia (gluc(-) cell groups), they remained more expressed in SD-hMSCs than in UP-hMSCs. Gluconeogenesis, a reverse glycolysis pathway, generates glucose from either pyruvate, OAA

or other small carbohydrate precursor sources and mainly occurs in specialized tissues, such as liver. Recent data, however, demonstrated that nonhepatic cancer cells express PEPCK-2 and may utilize some steps of gluconeogenesis to adapt to low-glucose conditions [46].

Another key result of this study is that, in the absence of both oxygen and glucose, SD-hMSCs use pyruvate to fuel their metabolism and sustain viability. Pyruvate can be metabolized through three major pathways in eukaryotic cells. First, pyruvate is converted into lactate catalyzed by lactate dehydrogenase. In our studies, however, no/minimal lactate was detected in the culture supernatants under ischemic conditions. Second, pyruvate is converted into acetyl-CoA to enter the TCA cycle. Acetyl-CoA may be further used for fatty acid synthesis and other anabolic pathways. In the absence of oxygen, however, the TCA cycle and related pathways are inhibited. Third, pyruvate may enter into the gluconeogenesis pathway. Taking into account our results, we hypothesize that SD-hMSCs cells may utilize at least some steps of gluconeogenesis to overcome the detrimental metabolic situation during glucose deprivation and anoxia. Further studies are needed to elucidate the exact underlying mechanisms and the downstream metabolic pathways of quiescence preconditioned hMSCs, for instance, using stable isotope-based metabolomic approaches in order to trace pathways and fluxes in cells.

CONCLUSION

Altogether, our findings demonstrated that, through a metabolic reprogramming not fully revealed yet, quiescence preconditioning by serum deprivation provides protective adaptation of hMSCs against abrupt transition to the deleterious ischemic environment. We speculate that, due to lower energy demands, quiescence preconditioned hMSCs adopt an oxygen-independent metabolic profile that appears favorable for withstanding the encountered metabolic stress. Rather than using a single pathway to ensure their survival under ischemia, SD-hMSCs likely use a multifaceted strategy to overcome this metabolic insult. Most importantly, quiescence preconditioning proved to be beneficial for hMSCs for at least 7 days postimplantation. For these reasons, this safe and easy-to-implement preconditioning appears as a promising, and to date untapped, strategy for stem cell therapies and tissue engineering applications.

ACKNOWLEDGMENTS

We thank Professor R. Bizios for critically reading the manuscript. We thank the St Louis hospital imaging facility for the fluorescence microscopy. We acknowledge the Centre National de la Recherche Scientifique (CNRS) and the Direction Générale de l'Armement (DGA) for the financial support of the study.

AUTHOR CONTRIBUTIONS

M.A.: Conception and design, collection and assembly of data, data analysis and interpretation, Manuscript writing, final approval of manuscript; L.N.: Collection and/or assembly of data, final approval of manuscript; P.J. and D.M.: Collection

and assembly of data, data analysis and interpretation; B.M.: provision of study material, data analysis and interpretation; I.V.: Collection and/or assembly of data; K.G.: Data analysis and interpretation, final approval of manuscript; P.H.: Conception and design, data analysis and interpretation, final approval of manuscript; L.-A.D.: Conception and design, data analysis

and interpretation, financial support, manuscript writing, final approval of manuscript.

CONFLICT OF INTEREST

The authors declare no potential conflict of interest.

REFERENCES

- Friedenstein AJ, Petrakova KV, Kurolesova AI et al. Heterotopic of bone marrow. Analysis of precursor cells for osteogenic and hematopoietic tissues. *Transplantation* 1968;6:230–247.
- Caplan AI. Adult mesenchymal stem cells for tissue engineering versus regenerative medicine. *J Cell Physiol* 2007;213:341–347.
- Giannoni P, Scaglione S, Daga A et al. Short-time survival and engraftment of bone marrow stromal cells in an ectopic model of bone regeneration. *Tissue Eng Part A* 2009;16:489–499.
- Liu J, Barradas A, Fernandes H et al. In vitro and in vivo bioluminescent imaging of hypoxia in tissue-engineered grafts. *Tissue Eng Part C Methods* 2010;16:479–485.
- Rodrigues M, Griffith LG, Wells A. Growth factor regulation of proliferation and survival of multipotential stromal cells. *Stem Cell Res Ther* 2010;1:32.
- Wu KH, Mo XM, Han ZC et al. Stem cell engraftment and survival in the ischemic heart. *Ann Thorac Surg* 2011;92:1917–1925.
- Beccourt P, Cambon-Binder A, Monfolet LE et al. Ischemia is the prime but not the only cause of human multipotent stromal cell death in tissue-engineered constructs in vivo. *Tissue Eng Part A* 2012;18:2084–2094.
- Haider H, Ashraf M. Strategies to promote donor cell survival: Combining preconditioning approach with stem cell transplantation. *J Mol Cell Cardiol* 2008;45:554–566.
- Patel ZS, Mikos AG. Angiogenesis with biomaterial-based drug- and cell-delivery systems. *J Biomater Sci Polym Ed* 2004;15:701–726.
- Pedersen TO, Blois AL, Xing Z et al. Endothelial microvascular networks affect gene-expression profiles and osteogenic potential of tissue-engineered constructs. *Stem Cell Res Ther* 2013;4:52.
- Wallner C, Schira J, Wagner JM et al. Application of VEGFA and FGF-9 enhances angiogenesis, osteogenesis and bone remodeling in Type 2 diabetic long bone regeneration. *PLoS One* 2015;10:e0118823.
- Niagara ML, Haider H, Jiang S et al. Pharmacologically preconditioned skeletal myoblasts are resistant to oxidative stress and promote angiomyogenesis via release of paracrine factors in the infarcted heart. *Circ Res* 2007;100:545–555.
- Wisel S, Khan M, Kuppusamy ML et al. Pharmacological preconditioning of mesenchymal stem cells with trimetazidine (1-[2,3,4-trimethoxybenzyl]piperazine) protects hypoxic cells against oxidative stress and enhances recovery of myocardial function in infarcted heart through Bcl-2 expression. *J Pharmacol Exp Ther* 2009;329:543–550.
- Deng J, Han Y, Yan C et al. Overexpressing cellular repressor of E1A-stimulated genes protects mesenchymal stem cells against hypoxia- and serum deprivation-induced apoptosis by activation of PI3K/Akt. *Apoptosis* 2010;15:463–473.
- Fan VH, Tamama K, Au A et al. Tethered epidermal growth factor provides a survival advantage to mesenchymal stem cells. *Stem Cells* 2007;25:1241–1251.
- Rodrigues M, Yates CC, Nuschke A et al. The matrikine tenascin-C protects multipotential stromal cells/mesenchymal stem cells from death cytokines such as FasL. *Tissue Eng Part A* 2013;19:1972–1983.
- Descheppe M, Manassero M, Oudina K et al. Pro-angiogenic and pro-survival functions of glucose in human mesenchymal stem cells upon transplantation. *Stem Cells* 2013;31:526–535.
- Descheppe M, Oudina K, David B et al. Survival and function of mesenchymal stem cells (MSCs) depend on glucose to overcome exposure to long-term, severe and continuous hypoxia. *J Cell Mol Med* 2011;15:1505–1514.
- Cheung TH, Rando TA. Molecular regulation of stem cell quiescence. *Nat Rev Mol Cell Biol* 2013;14:329–340.
- Friedenstein AJ, Chailakhyan RK, Gerasimov UV. Bone marrow osteogenic stem cells: in vitro cultivation and transplantation in diffusion chambers. *Cell and Tissue Kinetics* 1987;20:263–272.
- Logeart-Avramoglou D, Oudina K, Bourguignon M et al. In vitro and in vivo bioluminescent quantification of viable stem cells in engineered constructs. *Tissue Eng Part C Methods* 2010;16:447–458.
- Degat MC, Dubreucq G, Meunier A et al. Enhancement of the biological activity of BMP-2 by synthetic dextran derivatives. *J Biomed Mater Res* 2009;88:174–183.
- LoPiccolo J, Blumenthal GM, Bernstein WB et al. Targeting the PI3K/Akt/mTOR pathway: effective combinations and clinical considerations. *Drug Resist Updat* 2008;11:32–50.
- Gharibi B, Farzadi S, Ghuman M et al. Inhibition of Akt/mTOR attenuates age-related changes in mesenchymal stem cells. *Stem Cells* 2014;32:2256–2266.
- Qian W, Van Houten B. Alterations in bioenergetics due to changes in mitochondrial DNA copy number. *Methods* 2010;51:452–457.
- Coller HA, Sang L, Roberts JM. A new description of cellular quiescence. *PLoS Biol* 2006;4:e83.
- Winer JP, Janmey PA, McCormick ME et al. Bone marrow-derived human mesenchymal stem cells become quiescent on soft substrates but remain responsive to chemical or mechanical stimuli. *Tissue Eng Part A* 2009;15:147–154.
- Zhu W, Chen J, Cong X et al. Hypoxia and serum deprivation-induced apoptosis in mesenchymal stem cells. *Stem Cells* 2006;24:416–425.
- Potier E, Ferreira E, Meunier A et al. Prolonged hypoxia concomitant with serum deprivation induces massive human mesenchymal stem cell death. *Tissue Eng* 2007;13:1325–1331.
- Beegle J, Lakatos K, Kalomoiris S et al. Hypoxic preconditioning of mesenchymal stromal cells induces metabolic changes, enhances survival, and promotes cell retention in vivo. *Stem Cells* 2015;33:1818–1828.
- Manassero M, Paquet J, Descheppe M et al. Comparison of survival and osteogenic ability of human mesenchymal stem cells in orthotopic and ectopic sites in mice. *Tissue Eng Part A* 2016;22:534–544.
- Stegen S, van Gestel N, Eelen G et al. HIF-1 α promotes glutamine-mediated redox homeostasis and glycogen-dependent bioenergetics to support postimplantation bone cell survival. *Cell Metab* 2016;23:265–279.
- Gray JV, Petsko GA, Johnston GC et al. “Sleeping beauty”: Quiescence in *Saccharomyces cerevisiae*. *Microbiol Mol Biol Rev* 2004;68:187–206.
- Stuart JA, Brown MF. Energy, quiescence and the cellular basis of animal life spans. *Comp Biochem Physiol Part A Mol Integr Physiol* 2006;143:12–23.
- Folmes CD, Dzeja PP, Nelson TJ et al. Metabolic plasticity in stem cell homeostasis and differentiation. *Cell Stem Cell* 2012;11:596–606.
- Latil M, Rocheteau P, Chatre L et al. Skeletal muscle stem cells adopt a dormant cell state post mortem and retain regenerative capacity. *Nat Commun* 2012;3:903.
- Buttgereit F, Brand MD. A hierarchy of ATP-consuming processes in mammalian cells. *Biochem J* 1995;312:163–167.
- Boutillier RG. Mechanisms of cell survival in hypoxia and hypothermia. *J Exp Biol* 2001;204:3171–3181.
- Ochocki JD, Simon MC. Nutrient-sensing pathways and metabolic regulation in stem cells. *J Cell Biol* 2013;203:23–33.
- Valcourt JR, Lemons JM, Haley EM et al. Staying alive: Metabolic adaptations to quiescence. *Cell Cycle* 2012;11:1680–1696.
- Galluzzi L, Morselli E, Vicencio JM et al. Life, death and burial: multifaceted impact of autophagy. *Biochem Soc Trans* 2008;36:786–790.
- Mazure NM, Pouyssegur J. Hypoxia-induced autophagy: Cell death or cell survival? *Curr Opin Cell Biol* 2010;22:177–180.

43 Ito K, Suda T. Metabolic requirements for the maintenance of self-renewing stem cells. *Nat Rev Mol Cell Biol* 2014;15:243–256.

44 Buravkova LB, Andreeva ER, Gogvadze V et al. Mesenchymal stem cells and hypoxia:

where are we? *Mitochondrion* 2014;19: 105–112.

45 Folmes CD, Nelson TJ, Martinez-Fernandez A et al. Somatic oxidative bioenergetics transitions into pluripotency-dependent

glycolysis to facilitate nuclear reprogramming. *Cell Metab* 2011;14:264–271.

46 Leithner K, Hrzenjak A, Trotsmuller M et al. PCK2 activation mediates an adaptive response to glucose depletion in lung cancer. *Oncogene* 2015;34:1044–1050.



See www.StemCells.com for supporting information available online.